



X-ray observations and theoretical modeling of Active Galactic Nuclei
by Michael James Kellen

A thesis submitted in partial fulfillment of the requirements for the degree of Doctor of Philosophy in
Physics

Montana State University

© Copyright by Michael James Kellen (1997)

Abstract:

The archival ASCA observation of the Seyfert 1 galaxy NGC 4593 is thoroughly analyzed across the entire calibrated X-ray band. In addition to the typical power law spectrum, several emission and absorption features are discovered. Temporal analysis of several of these features indicates significant variability in correlation to the variations in the continuum luminosity and each other. Several possible models are put forth to describe the spectrum.

A self-consistent one dimensional nonthermal pair plasma disk-corona model for the high energy spectrum of active galaxies is developed following the intent of earlier work. The detailed physics is used along with object oriented programming techniques to implement a library of pair plasma object routines, which are tested and used to explore the behaviour of a pair-plasma atmosphere.

X-RAY OBSERVATIONS AND THEORETICAL
MODELING OF ACTIVE GALACTIC NUCLEI

by

Michael James Kellen

A thesis submitted in partial fulfillment

of the requirements for the degree

of

Doctor of Philosophy

in

Physics

MONTANA STATE UNIVERSITY

Bozeman, Montana

July 1997

D378
K2809

ii

APPROVAL

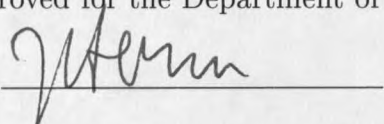
of a thesis submitted by

Michael James Kellen

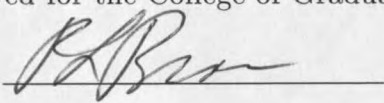
This thesis has been read by each member of the thesis committee and has been found to be satisfactory regarding content, English usage, format, citations, bibliographic style, and consistency, and is ready for submission to the College of Graduate Studies.

Sachiko Tsuruta  7/10/97
(Signature) Date

Approved for the Department of Physics

John Hermanson  7-10-97
(Signature) Date

Approved for the College of Graduate Studies

Robert L. Brown  7/27/97
(Signature) Date

©COPYRIGHT

by

Michael Kellen

1997

All Rights Reserved

STATEMENT OF PERMISSION TO USE

In presenting this thesis in partial fulfillment of the requirements for a doctoral degree at Montana State University-Bozeman, I agree that the Library shall make it available to borrowers under rules of the Library. I further agree that copying of this thesis is allowable only for scholarly purposes, consistent with "fair use" as prescribed in the U.S. Copyright Law. Requests for extensive copying or reproduction of this thesis should be referred to University Microfilms International, 300 North Zeeb Road, Ann Arbor, Michigan 48106, to whom I have granted "the exclusive right to reproduce and distribute my dissertation in and from microform along with the non-exclusive right to reproduce and distribute my abstract in any format in whole or in part."

Signature _____



Date _____

7/23/97

ACKNOWLEDGEMENTS

I would like to thank Professor Sachiko Tsuruta for her support and guidance in my graduate career. Professor Hideyo Kunieda, Doctor Karen Leighly and Professor Richard Mushotzky have each provided invaluable instruction in the art of data analysis. Anna LeRoux has provided me with many chances to pass some of that on and so help me to understand it better, as well as putting up with my hogging all of the computer time.

On a personal level, I must credit it all to my loving parents, who taught me that most valuable of lessons, to want to learn. Far too many others have supported and comforted me in this task for me to name them all here. You and I know who you are.

Contents

1	INTRODUCTION	1
1.1	The Active Galaxy	2
1.1.1	History	2
1.1.2	The Active Galaxy Zoo	3
1.1.3	Seyferts	5
1.2	The Heart of the Matter	6
1.2.1	Size and Energy	7
1.2.2	Gross Properties of the X-ray Emission	9
1.2.3	High Energy Spectral Features	11
1.3	The Central Engine	12
1.3.1	Popular Conclusions	12
1.3.2	The "Standard Model"	16

1.3.3	Nonstandard Problems	21
1.4	Non-homogeneous Modeling	22
1.4.1	Models To-date	23
1.4.2	Model to be presented	24
1.5	Back in the Real World	25
2	ANALYSIS OF NGC 4593	26
2.1	Notes on Statistics	27
2.1.1	Chi-Squared: Gaussian Noise	27
2.1.2	The C Statistic: Poisson Noise	29
2.1.3	Confidence Ranges	30
2.1.4	The Right Tool	31
2.2	Previous Analyses	32
2.3	The Observation	33
2.4	Timing Analysis	35
2.5	Spectral Analysis	38
2.5.1	Background	39
2.5.2	The Hard X-ray Spectrum	42
2.5.2.1	Power Law	45
2.5.2.2	High Energy Tail	48

2.5.2.3	Iron Line	56
2.5.3	The Soft X-ray Spectrum	61
2.5.3.1	Galactic Hydrogen Absorption	61
2.5.3.2	A Possible Soft Emission Line	63
2.5.3.3	Soft X-ray Absorption Features	67
2.5.3.4	An Alternate View	72
2.6	Summary & Discussion of Our Results	73
3	ELECTRON-POSITRON/PHOTON PHYSICS	81
3.1	Radiation Processes	82
3.1.1	Compton Scattering	82
3.1.2	Bremßstrahlung Radiation	85
3.1.3	Synchrotron Radiation	90
3.1.4	Absorption & Optical Depth	92
3.1.5	Photoionization and Fluorescence	93
3.2	The Pair Plasma	96
3.2.1	Pair Annihilation	96
3.2.2	Pair Creation	99
3.3	Nonthermal Cascades	101
3.4	Previous Work	102

3.5	Current Advancements	105
4	BATH	108
4.1	A Conceptual Overview	109
4.2	Details	112
4.2.1	Photon Source Function	114
4.2.2	Reaction Rate Function	116
4.2.3	The Code	118
4.3	Reality Checks	121
4.3.1	The SHOWER Limit	122
4.3.2	The Thermal Limit	122
4.3.3	The Monte Carlo Limit	125
4.4	Results and Constraints	126
4.4.1	Input Dependencies	127
4.4.2	Annihilation Radiation	132
4.4.3	The Gamma-Ray Background	134
4.4.4	X-ray Power Law	138
4.4.5	Upon Reflection	140
4.4.6	The 100 keV Break	142
4.5	Discussion	144

5 CONCLUSIONS	146
5.1 Introduction	146
5.2 Observation	147
5.3 Particle Theory	148
5.4 Computational Model	149
5.5 Concluding Remarks	150
Bibliography	152
APPENDICES	162
A. Exact Compton Scattering Photon Distribution	162
B. Differential Cross-section of $e^{\pm}e^{\pm}$ Bremsstrahlung	163
C. C++ Header files for BATH	166

List of Tables

2.1	Relation of Confidence to the Change of Statistic	30
2.2	Fitting Parameters for the hard X-ray power law	49
2.3	Fit parameters for the Broken Power Law model	51
2.4	Ionized Reflection Model Fit Parameters	53
2.5	Partial Covering Fit Parameters	55
2.6	Fitting Parameters for iron K line.	60
2.7	Oxygen VI Emission Line Fit	65
2.8	Parameters of fit using two absorption edges	69
2.9	Ionized absorber model fit parameters	70

List of Figures

1.1	Multiwavelength Spectrum of a radio quiet active galaxy (after Schlickeiser, 1980)	7
1.2	Schematic of the "Standard Model" for active galaxies	17
1.3	Dust Torus in NGC 4261.(Jaffe, <i>et al.</i> , 1993)	19
1.4	Ionization cones in NGC 5728	20
2.1	The light curve of NGC 4593, binned in 8192 second intervals.	35
2.2	Light curve in various X-ray bands	37
2.3	SAOimage plot indicating object and near sky background regions	40
2.4	The Diffuse X-ray background. NGC 4593 at center.	41
2.5	Comparison of detectors, with and without backgrounds	43
2.6	Background Spectra for the different methods	44

2.7	A power law fit to the data.	46
2.8	χ^2 residuals after high energy fit (rebinned for clarity)	57
2.9	High and Low State iron Line Normalization Contours	59
2.10	The X-ray spectrum shown with the hard X-ray model.	62
2.11	Soft X-Ray Residuals showing several features	64
2.12	Confidence contours of Powerlaw v. OVI Gaussian	66
2.13	Ratio of the observed soft x-rays to the model.	68
2.14	Ionization parameter confidence contours	71
2.15	Fractional Changes in Absorption Edge Depth	74
2.16	Model Spectra for Ionized Absorber and <i>ad hoc</i> Lines and Edges	80
3.1	Results from Tritz, 1990 (solid) and Tsuruta & Kellen, 1995 (dashed)	107
4.1	Comparison between SHOWER and BATH without backward scattering	123
4.2	BATH results in the limit of no hard photon source	124
4.3	Comparison of BATH to Tritz's (P1+P2) Method	126
4.4	Insensitivity to the input spectral shape	129
4.5	Variations in source layer altitude	131

4.6	Results for varying compactness values	133
4.7	Equivalent width of the Annihilation line in several models . .	135
4.8	Ratio of Gamma-Ray production to observed background . . .	137
4.9	Power Law Fits to Model Output	139
4.10	X-ray Compactness Ratios from Model	141

ABSTRACT

The archival ASCA observation of the Seyfert 1 galaxy NGC 4593 is thoroughly analyzed across the entire calibrated X-ray band. In addition to the typical power law spectrum, several emission and absorption features are discovered. Temporal analysis of several of these features indicates significant variability in correlation to the variations in the continuum luminosity and each other. Several possible models are put forth to describe the spectrum.

A self-consistent one dimensional nonthermal pair plasma disk-corona model for the high energy spectrum of active galaxies is developed following the intent of earlier work. The detailed physics is used along with object oriented programming techniques to implement a library of pair plasma object routines, which are tested and used to explore the behaviour of a pair-plasma atmosphere.

Chapter 1

INTRODUCTION

We begin with a review of the current observational and theoretical state-of-the-art in the study of the central engines of Active Galactic Nuclei (AGNs). First, we will present the definition and observational history of AGN. From there we will narrow our focus to the high energy central engines of these objects and the associated X-ray emissions. Next we will present currently viable theoretical models of the physical processes in the central engine and discuss their strengths and shortcomings. We shall then present an additional model which attempts to address these shortcomings.

1.1 The Active Galaxy

We review the discovery of the various varieties of active galaxies and how they are differentiated. Some of the more interesting problems in understanding them are pointed out. There are several features which are commonly accepted as distinguishing 'active' galaxies from 'normal' ones:

- A compact, bright galactic nucleus
- Rapid variations in luminosity
- A strong nonstellar continuum

The criterion of compactness is not always applied. Radio-loud active galaxies (discussed in section 1.1.2) are dominated by regions of radio emission which extend far outside the host galaxy.

1.1.1 History

Many radio sources were discovered in the late 1940s, but with the identification of a radio source with the extragalactic optical source Cygnus A (Baade & Minkowski, 1954), multiwavelength observations of active galaxies became a vital tool. Active galaxies have been observed in all wavelengths now, up to and including TeV (yes, erg!) gamma rays (T.C. Weekes, 1996).

The variability of some AGNs was used by Matthews & Sandage (1963) to place the first limits on the size of the optical emission region. The variability on time scales of weeks requires scales of light-weeks or less (by causality arguments). The energy density calculated from this scale and the observed luminosity made it impossible for this energy to be stellar in origin. Later discovery of intraday variations (Oke, 1967) pushed these energy densities still higher.

An early discovery in the field of X-ray astronomy was that much of the luminosity of active galaxies is emitted in the X-ray band (Elvis, *et al.*, 1978). This is in fact such a common feature of AGN that it can almost be considered a criterion for being "active".

1.1.2 The Active Galaxy Zoo

Active galaxies are often divided into two categories based upon their relative radio luminosity. These classes are radio loud and radio quiet. Radio loud active galaxies appear to have multiple sources of radio energy, generally a radio quiet "core" with an additional luminous, extended region of emission (Antonucci, 1993).

Radio loud objects can also be classified by the physical location of the

radio source relative to the galaxy. Some radio loud galaxies display kilo- to megaparsec scale lobes of radio emission, some symmetric, some distorted (apparently by the local intergalactic medium) (Jennison & Das Gupta, 1953). These galaxies are referred to as lobe-dominated. Other radio loud galaxies emit most of their radio luminosity from a small region close to the core of the galaxy. These are referred to as core-dominated.

Core-dominated radio loud active galaxies show a highly variable and polarized optical-near IR component. If this component dominates other optical spectral features, the object is referred to as a BL Lac object. If the spectrum sometimes displays broad emission lines, the object is classified as an Optically Violently Variable quasar (OVV). Both categories are collectively referred to as *blazars* (attributed to Spiegel, see Angel & Stockman, 1980). This optical/IR component is understood to be the high energy tail of the core radio process (Landau, *et al.*, 1986).

Lobe-dominated radio loud active galaxies, as well as radio quiet active galaxies, can be further subdivided into two types. Type 2 galaxies have spectra which show narrow permitted and forbidden emission lines. Line widths are usually of < 1000 km/s. Type 1 galaxies show additional broad emission lines with widths on the order of 10,000 km/s. The relative line strengths in

type 1 galaxies indicate that optical depth effects are often important. Type 1 galaxies also have strong, variable nonthermal continua.

The lower luminosity (*ie*, closer) active galaxies can be seen to be spirals. These are classified as Seyfert galaxies, discussed in the next section. Higher luminosity AGN (usually at greater distances) can sometimes be identified as ellipticals, and are referred to as quasars (QSOs). It has also been argued that ultraluminous infrared galaxies are in fact highly luminous Type 2's, which are otherwise underrepresented.

Galaxies at the lowest "active" limit of core luminosity are Low Ionization Nuclear Emission Regions (LINER)s (Heckman, 1980). These are spirals which show some variable nuclear emission features. Photoionization models developed for Seyfert galaxies have been successfully applied (with lower ionization parameters) to these objects (Ferland & Netzer, 1983), suggesting that they are the weakest objects in the extended family of active galaxies.

1.1.3 Seyferts

Seyfert galaxies are defined in two general classes (Seyfert, 1943). Type 1 Seyferts are spiral galaxies with bright, point-like nuclei in the optical and X-ray bands. They have broad permitted emission line features in their

spectra in the optical and UV ($\delta v \geq 3000$ km/sec). Their optical continuum is dominated by nonthermal emission. Type 2 Seyferts show strong, narrow ($200 < \delta v < 2000$ km/sec) forbidden emission lines instead of the broad lines of the Type 1's. They also have little or no nonthermal component to their optical spectrum.

These two classes are not, in practice, quite so distinct. In fact, as we shall discuss later, most (but not all) of the differences can be reconciled with a single physical model. Several "transitional" classes are sometimes assigned (1.5, 1.8 and 1.9) based upon the relative strengths of the broad and narrow line components (Osterbrock & Matthews, 1986).

1.2 The Heart of the Matter

AGN are visible at many scales and in many parts of the electromagnetic spectrum. By studying the similarities and differences shown by different classes of active galaxies, we can try to formulate a model of the physical processes which drive them.

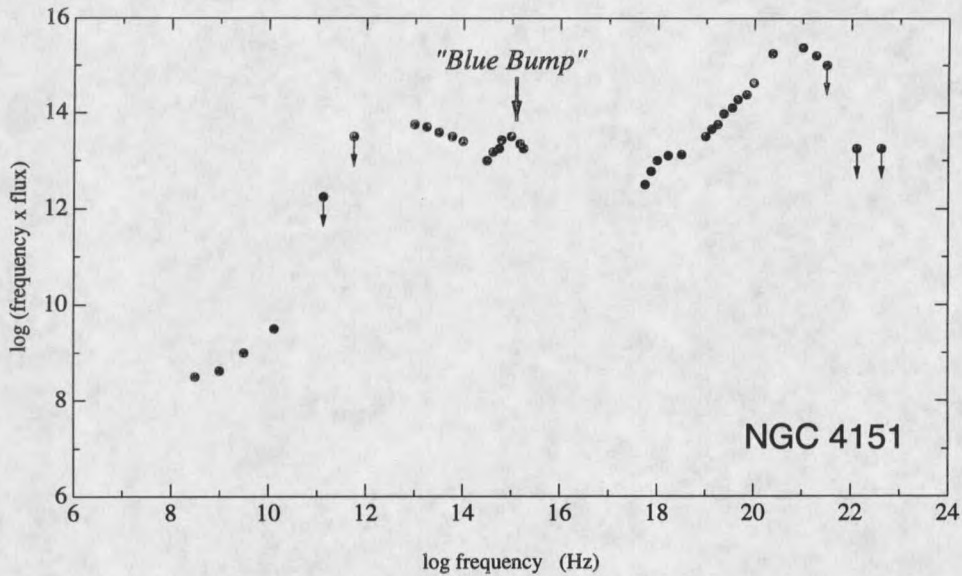


Figure 1.1: Multiwavelength Spectrum of a radio quiet active galaxy (after Schlickeiser, 1980)

1.2.1 Size and Energy

The intimate relationship between wavelength and energy allow us to use different wavelengths of light to study different scales in an AGN. The highest energies are emitted very close to the central engine, and so can be used to probe it. The rapid variations seen in the high energy emissions imply large scale changes on the order of hours or days, with correspondingly small characteristic distances determined by the light travel time.

Figure 1.1 shows the spectrum of a radio-quiet AGN from the radio to the hard X-ray. The x-axis indicates the log of the frequency, while the y-axis

indicates the log of the frequency times the flux at that frequency. These axes are chosen because the resulting plot has the property that equal areas under a curve represent equal luminosities. Equivalently, a horizontal line would indicate that equal amounts of energy are being emitted at each wavelength. One can also rescale the graph into units of log photon energy and log of photon energy times the flux at that energy without changing the shape of the plotted data.

In the optical and ultraviolet, we often see rapid variability (Optically Violently Variables being the most obvious example) as well as strong spectral features. In addition to Hydrogen emission lines, the visible-UV region of radio-quiet AGNs contains an excess of photons relative to the generally power law nature seen in other wavelengths. This so-called "blue bump" (indicated on the figure) can be fit by a thermal profile of a few tens of thousands of Kelvins (Pringle, 1981). Also visible in the optical are narrow linear structures referred to as jets (Curtis, 1918). These structures extend on the parsec scale in the visible.

Radio observations, on the other hand, are often used to study the kilo- to megaparsec scale radio jets and lobes of the radio-loud active galaxies (Miley, 1980). It should be stressed that the radio luminosity can be of roughly the

same order as that in higher energy bands, but is likely generated *in situ* by relativistic particles in a strong magnetic field (Wardel, et al., 1986; Jones, 1988; Begelman, et al., 1984).

1.2.2 Gross Properties of the X-ray Emission

The general character of the X-ray emission from active galaxies seems to fall into two categories, radio-loud and radio-quiet. Those AGN which are classified as radio-loud have stronger X-ray emission as well (Worall, *et al.*, 1987). Their spectra tend to lack the detailed features at higher energies (> 6 keV). In the unified model presented in section 1.3.2, we shall discuss the possible relation of relativistic jets of material to the distinction between these two types.

The X-ray emissions of radio-quiet AGN are characterized by rapid, high amplitude variability (Snyder, *et al.*, 1980). Changes happen on the order of days, hours (Tennant & Mushotzky, 1983) or even minutes (Kunieda, *et al.*, 1990) and be of very large amplitudes ($\delta I/I \sim 1$). They are also highly luminous in the X-ray, with 5-40% of their bolometric luminosity being emitted in this region of the spectrum (Ward, *et al.*, 1987).

The spectral shape of these radio-quiet AGN in the X-ray from 2-20 keV

has been known to be roughly a power law since the late 70's (Mushotzky, 1978a,b; Ives, *et al.*, 1976; Stark, *et al.*, 1977). These observations also showed the first detections of iron K-line (6.4 keV) emission. Samples with larger numbers of objects have since found that both of these features are common to radio-quiet AGN and that the photon spectral index is narrowly clustered around $\Gamma = 1.7$ (Mushotzky, *et al.*, 1980). The fact that less energy is observed at the lower end of the power law is attributed to absorption by a column of neutral Hydrogen:

$$N(E) = \text{const.} \times E^{-\Gamma} \times e^{-\sigma(E)N_H} \quad \text{photons/s/cm}^2/\text{keV} \quad (1.1)$$

where N_H is the column density and $\sigma(E)$ is the effective cross-section for neutral Hydrogen atoms.

These findings have continued to be seen as the observations have been extended and improved. Observations using the *Ginga* Large Area Counter (LAC) have shown that a significant fraction of all Seyferts have Fe K line features far in excess of the level to be expected from material in the line of sight (Matsuoka, *et al.*, 1990; Pounds, *et al.*, 1989; Nandra, 1991).

The *Ginga* spectra also showed a flattening in the power law spectrum above 8 keV in about 40% of observed Seyferts (Nandra, 1991). This has been

attributed to reprocessing of the intrinsic emitted spectrum by additional cold gas which either partially covers or reflects the incident spectrum (Guilbert & Rees, 1988; Lightman & White, 1988).

With the advent of *ASCA*, additional features have begun to be seen in the X-ray spectra. In particular, absorption and emission features in the soft X-ray (.5-1 keV) range have been seen in some objects. In a few objects, these features are even seen to be varying relative to the continuum. (George, *et al.*, 1997)

1.2.3 High Energy Spectral Features

Recent (OSSE) observations of the higher energy spectra of Seyfert galaxies (Madjeski, *et al.*, 1995; Zdziarski, *et al.*, 1995) have been used to place limits upon the shape of the X-ray spectrum of Seyferts above about 100 keV. The best fits found to these observations require an exponential cut-off in the power law at about 100-150 keV.

The same studies have placed upper limits upon the strength of any electron-positron annihilation line in the spectra of Seyferts. Nondetection requires that the generated line have an equivalent width of less than 300 keV.

1.3 The Central Engine

In attempting to understand the physical processes taking place in the central engine of AGNs, we are not faced with a completely blank slate. There are constraints upon the possible models placed by observational evidence as well as purely physical reasons to prefer one model to another.

1.3.1 Popular Conclusions

The natural curiosity associated with such a strong energy source with such a small characteristic size has made theorizing about the central engine of active Galaxies a major passtime for extragalactic astronomers. For some time, theoretical arguments from several sources (see, for example, Salpeter, 1964) have suggested that mass accretion onto supermassive black holes could be the explanation.

In addition to scale arguments, which push the energy densities beyond simple stellar generation, the observations of highly relativistic, even “superluminal” jets of material suggest relativistically compact generators (Bridle & Pearley, 1984). Accretion efficiencies and AGN luminosities predict black hole masses from between 10^6 and $10^{9.5} M_{\odot}$. Unfortunately, AGN are much less common now (at $z \leq 1$) than they have been in the past ($z \geq 2$). This

implies many dead or dormant AGN engines in nearby galaxies.

Rees (1996) presents several compelling observational arguments for the existence of supermassive black holes in the nuclei of other galaxies. The strongest is the precise mapping of gas motions in the core of NGC 4258 by observing maser emission from H_2O . The 1.3 cm emission can be resolved to within 1 km/sec and angular resolution better than 0.5 milliarc seconds. The observed rotational speeds describe Keplerian motion around a central mass of $3 \times 10^7 M_\odot$ (Watson & Wallin, 1994; Miyoshi, *et al.*, 1995).

Ford, *et al.* (1994) detected an orbiting disk of hot gas in M87 with rotational speeds of about 550 km/s, which requires a central mass on the order of $3 \times 10^9 M_\odot$. This is a much higher mass than can be accounted for by the observed stars in the inner region. Recent Hubble Space Telescope Imaging Spectrograph (STIS) observations have fairly conclusively detected the doppler signature of a supermassive black hole in the core of M84 (Bower, *et al.*, 1997). With rotational velocities of over 400 km/s within 26 light years of the central mass and clearly Keplerian motion, the calculated central mass is $3 \times 10^8 M_\odot$. This supplements an earlier survey of 27 nearby galaxies which detected massive black holes in three nearby normal galaxies (NGC 3379 (also known as M105), NGC 3377 and NGC 4486B, a companion galaxy to

M87) and concluded that massive (million or more M_{\odot}) black holes may exist in every galaxy, and that they may be an inevitable product of formation (Gebhardt, *et al.*, 1997). Radio observations of our own Galactic Center indicate a high mass central object ($\sim 10^6 M_{\odot}$ in the inner $\sim .1$ A.U.), with an orbiting disk or torus of gas and a thick molecular torus at a distance of about 200 pc (Morris & Serabyn, 1996). The interested reader is directed to the *Annual Review* article by Kormendy and Richstone (1995) for a more detailed discussion.

The existence of the iron fluorescent emission line at 6.4 keV implies a relatively large amount of nearly neutral material. The equivalent width (EW) of this line is sometimes quite broad ($50 < \text{EW} < 350$ eV) (Nandra, 1991). A thermal emission line at 6.7 keV can usually be excluded. The strength of the line requires that much of the solid angle seen by the source must be occupied by high column density gas ($> 10^{22}$ atoms/cm²) (George & Fabian, 1991).

By combining 12 *Ginga* spectra to increase the signal-to-noise, Pounds, *et al.* (1990) found a flattening of the X-ray spectral slope above about 10 keV. They also found evidence in some Seyferts for an absorption feature from ionized iron above 7 keV. Two major theories have been put forth to

explain these features, with the distinction being primarily one of viewing angle.

One possibility is that the intrinsic spectrum is reflected by an optically thick medium which covers a large solid angle for the source (Lightman & White, 1988; Guilbert & Rees, 1988; George & Fabian, 1991). The reflection is strongest at higher energies, because of the ionization energies of the medium. Above the energy of the iron absorption edges (around 7-9 keV), the reflection increases to peak at about 20-30 keV before being curtailed by Compton down-scattering and reduced opacity at higher energies. This model is attractive on several levels. We have a ready-made reflector, that being the accretion disk of the central black hole. The reflection process provides a method of exciting fluorescence of the iron line, as well as the depletion seen at 7-8 keV, due to the reduced reflectivity near the ionization edges of iron. Fits based upon this model find a steeper intrinsic X-ray power law ($\Gamma \sim 1.9$). The lower value which has been found observationally is attributed to our inability to resolve the high energy flattening until recently (Pounds, *et al*, 1990; Nandra, 1991).

The other possibility is that of partial covering of the source. If there is material which irregularly and incompletely obscures the line of sight, much

of the flux below 6 keV will be absorbed by the high column densities. Iron line fluorescence as well as iron absorption features in excess of those to be expected from the softer energy results are a by-product of this model. In this case, the intrinsic power law is reduced in flux below 6 keV, creating a “flattening” which is in fact due to the diminishing opacity at higher energies. A physical model which provides a source for this absorber involving spherical accretion was put forth by Sivron & Tsuruta (1993) and discussed in detail in Sivron (1995).

1.3.2 The “Standard Model”

An idealized model of active galaxies which unifies many of the different types has arisen from many sources, as summarized in Antonucci (1993). The differences in spectral features and variability are put forward to be due to differences in the orientation of a nonspherical system.

The so-called Standard Model is illustrated in Figure 1.2. It consists of a central engine, implicitly assumed to be a massive black hole with an accretion disk in the inner milliparsec or so of the galaxy. This engine is the source of our nonthermal continuum and our visible-UV excess (“blue bump”). This strong energy source also drives the broad emission lines,

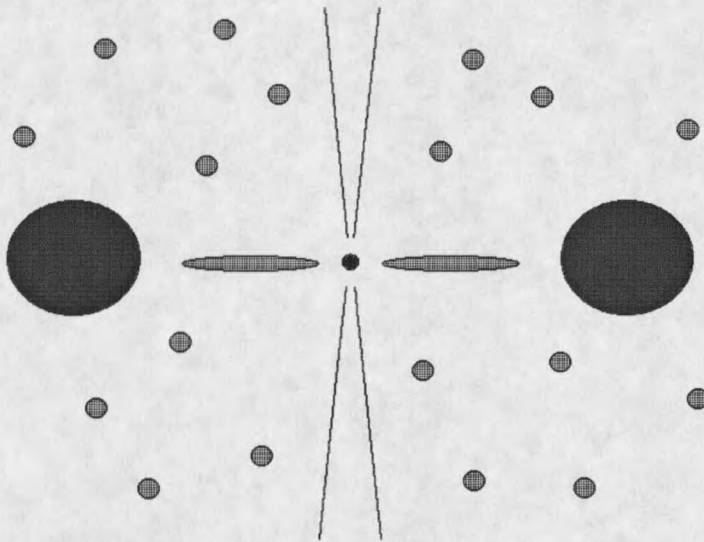


Figure 1.2: Schematic of the “Standard Model” for active galaxies

which are generated in the surrounding gas at about .1 to 1 pc from the engine. In addition to this, an optically thick torus is located at a greater distance (hundreds of parsecs) and roughly coplanar with the accretion disk, which obscures the central engine from certain lines of sight. Other, smaller, molecular clouds are posited to be scattered throughout the 10 to 100 parsec scale region to explain narrow emission line features. If the object exhibits a polar jet, that feature can be included in this model, and in fact is invoked in some cases as being nearly along the line of sight as an explanation of a highly variable and featureless spectrum, such as that seen in blazars.

These features are not simply pulled out of thin air. The reasonability of the black hole/accretion disk system was discussed earlier. The other major feature is the obscuring torus. This element has been derived historically from the attempt to unify the different types of Seyfert galaxies, but as we have seen, the distinction between Seyferts and other types of active galaxies has become blurred as observations have improved.

The lack of broad emission lines and weak to nonexistent featureless optical continua of Seyfert 2's can be attributed to one of two possibilities: either they are not present, or they are obscured from view. The latter possibility is the one which has been better supported by other evidence. Excesses of dust (IR) emission (Rowan-Robinson, 1977) support the existence of optically thick dust in some objects. More recently, Hubble Space Telescope observations show aligned dusty tori in some LINERs. Figure 1.3 shows the central few parsecs of NGC 4261 as seen by the HST. The detail image clearly shows a disc structure. Other observers have noted that the extrapolated nonthermal continuum is insufficient to generate the observed Ly α flux, implying that the narrow line emitting gas must be exposed to ionizing flux not visible to us (Neugebauer, *et al.*, 1980).

One final argument for this unifying model is based on NGC 1068. While

